

EFFECT OF RADIATION ABSORPTION AND NON UNIFORM HEAT SOURCE ON HYDRO MAGNETIC CONVECTIVE HEAT AND MASS TRANSFER FLOW OF CHEMICALLY REACTING FLUID PAST A STRETCHING WITH THERMOPHORESIS

K.Kalpana¹ and Dr.M.Sreevani²

¹Research scholar in Mathematics, Rayalaseema University, Kurnool, A.P

²Assistant Professor, Mathematics, S.K.University, Anantapur, A.P

Abstract

We discuss the combined influence of thermo-diffusion and radiation absorption effects on unsteady MHD heat and mass transfer flow of a viscous incompressible chemically reacting fluid over a stretching sheet with thermal radiation, non-uniform heat source/sink and thermophoresis particle deposition. The nonlinear governing equations have been solved by employing Galerkin finite element technique with quadric approximation function. The effect of radiation absorption, chemical reaction, hall effects and thermophoresis on all the flow characteristics have been represented graphically.

Keywords : Radiation absorption, chemical reaction, hall effects, sores effect, and non uniform heat source.

1. INTRODUCTION

In industry, polymer sheets and filaments are manufactured by continuous extrusion of the polymer from a die. The thin polymer sheet constitutes of continuously moving surface with a non-uniform velocity through an ambient fluid. The problem of heat and mass transfer flow due to stretching sheet has been implemented on many flow situations. The problem of steady two dimensional viscous incompressible fluid caused by a stretching sheet was first examined by Sakiadis [19]. The thermal behavior of the problem was experimentally verified by Tsou et al [23]. Crane [5] has studied the flow past a stretching plate by taking velocity varying linearly with a distance from a fixed point and this problem is the extension of Sakiadis[19]. Gupta et al. [10] have studied heat and mass transfer characteristics of stretching sheet with suction or blowing. Grubka and Bobba [9] studied the heat transfer characteristics over a continuous stretching surface with variable temperature. Ali [2] has investigated flow a heat transfer characteristics on a continuous stretching surface using power-law velocity and temperature distributions. Vajravelu [25] has analyzed the study of flow and heat transfer in saturated porous medium over an impermeable stretching sheet. Two cases have been discussed in this problem, (i) the sheet with prescribed sheet temperature (PST-case) and (ii) the sheet with prescribed wall flux (PHF-case).

In all the previous investigations, the effects thermal radiation and magnetic field on the flow and heat transfer have not been studied. It is well known the radiative heat transfer flow is very important in manufacturing industries for the design of reliable equipment's, nuclear plants, gas turbines and various propulsion devices for aircraft, missiles, satellites and space vehicles. Also, the effects of thermal radiation on forces and free convection flow are important in the content of space technology and process involving high temperature. This is due to the fact that the magnetic nanoparticles are regarded more adhesive to tumor cells than non-malignant cells. Such particles absorb more power than micro particles in alternating

current magnetic fields tolerable in humans i.e. for cancer therapy, Plumb et al. [17] was the first to examine the effect of horizontal cross flow and radiation on natural convection from vertical heated surface in a saturated porous media. Pal D et. al [15] has discussed radiation effect on hydro magnetic Darcy Forchheimer mixed convection flow over stretching sheet. Mansour and El-Shaer [13] analyzed the effects of thermal radiation on magneto hydrodynamic natural convection flows in a fluid saturated porous media. Pal [16] studied heat and mass transfer in stagnation-point flow toward a stretching sheet in the presence of buoyancy force and thermal radiation. Vajravelu and Rollins [24] studied heat transfer in electrically conducting fluid over a stretching sheet by taking into account of magnetic field only. Molla et al. [14] studied the effect of thermal radiation on a steady two-dimensional natural convection laminar flow of viscous incompressible optically thick fluid along a vertical flat plate with stream wise sinusoidal surface temperature. Abo-Eldahab and El-Gendy [1] investigated the problem of free convection heat transfer characteristics in an electrically conducting fluid near an isothermal sheet to study the combined effect of buoyancy and radiation in the presence of uniform transverse magnetic field.

In recent years, it is found that thermophoresis is a phenomenon has many practical applications in removing small particles from gas streams, in determining exhaust gas particle trajectories from combustion devices, and in studying the particulate material deposition on turbine blades. It has been found that thermophoresis is the dominant mass transfer mechanism in the modified chemical vapor deposition (MCVD) process as currently used in the fabrication of optical fiber performs. Thermophoretic deposition of radioactive particles is considered to be one of the important factors causing accidents in nuclear reactors. A number of analytical and experimental papers in thermophoretic heat and mass transfer have been communicated. Talbot et al [22] presented a seminal study, considering boundary layer flow with thermophoretic effects, which has become a benchmark for subsequent studies. Several authors, Duwairi and Damseh et al [8], Damseh et al [6], Mahdy and Hady [11], have investigated the effect of thermophoresis in vertical plate, micro-channel, horizontal plate and parallel plate.

As many industrially and environmentally relevant fluids are not pure, it has been suggested that more attention should be paid to convective phenomena which can occur in mixtures, but are not in common liquids such as air or water. Applications involving liquids mixtures include the costing of alloys, ground water pollutant migration and separation operations. In all of these situations, multi component liquids can undergo natural convection driven by buoyancy force resulting from simultaneous temperature and species gradients. In the case of binary mixtures, the species gradients can be established by the applied boundary conditions such as species rejection associated with alloys costing, or can be induced by transport mechanism such as Soret (thermo) diffusion. In the case of Soret diffusion, species gradients are established in an otherwise uniform concentration mixture in accordance with Onsager reciprocal relationship. Thermal-diffusion known as the Soret effect takes place and as a result a mass fraction distribution is established in the liquid layer. The sense of migration of the molecular species is determined by the sign of Soret coefficient. Soret and Dufour effects are very significant in both Newtonian and non-Newtonian fluids when density differences exist in flow regime. The thermo-diffusion (Soret) effect is corresponds to species differentiation developing in an initial homogeneous mixture submitted to a thermal gradient and the diffusion thermo (Dufour) effect corresponds to the heat flux produced by a concentration gradient. Usually, in heat and mass transfer problems the variation of density with temperature and concentration give rise the a combined buoyancy force under natural convection and hence the temperature and concentration will influence the diffusion and energy of the species. Many papers are found in literature on Soret and Dufour effects on different geometries. Dulal Pal et al [7] has studied MHD non-Darcian mixed convection heat

and mass transfer over a non-linear stretching sheet with Soret and Dufour effects and chemical reaction. MHD mixed convection flow with Soret and Dufour effects past a vertical plate embedded in porous medium was studied by Makinde [12], Reddy et al. [18] has presented finite element solution to the heat and mass transfer flow past a cylindrical annulus with Soret and Dufour effects. Chamkha et al. [4] has studied the influence of Soret and Dufour effects on unsteady heat and mass transfer flow over a rotating vertical cone and they suggested that temperature and concentration fields are more influenced with the values of Soret and Dufour parameter.

In all the above studies the physical situation is related to the process of uniform stretching sheet. For the development of more physically realistic characterization of the flow configuration it is very useful to introduce unsteadiness into the flow, heat and mass transfer problems. The working fluid heat generation or absorption effects are very crucial in monitoring the heat transfer in the regions, heat removal from nuclear fuel debris, underground disposal of radiative waste material, storage of food stuffs, exothermic chemical reactions and dissociating fluids in packed-bed reactors. This heat source can occur in the form of a coil or battery. Very few studies have been found in literature on unsteady boundary flows over a stretching sheet by taking heat generation/absorption into the account. Wang [26] was first studied the unsteady boundary layer flow of a liquid film over a stretching surface. Sreeniva Reddy [21] has discussed the effect of thermoporosis on unsteady mixed convective heat and mass transfer flow past stretching sheet with thermal radiation, Soret and Dufour effect in the presence of non uniform heat source. Aliveni et al [3] have discussed Soret and Dufour effects on convective heat and mass transfer flow of a viscous fluid in the presence of thermophoresis deposition particle. Sivagopal et al [20] have discussed Soret and Dufour effects on MHD heat and mass transfer flow of a micropolar fluid over stretching sheet through porous medium with thermophoresis.

In this paper, we analyze the combined influence of thermo-diffusion and radiation absorption effects on unsteady heat and mass transfer flow of a viscous incompressible electrically conducting fluid over a stretching sheet with thermal radiation, non-uniform heat source/sink and thermophoresis particle deposition. The nonlinear governing equations have been solved by employing Galerkin finite element technique with quadric approximation function. The effect of radiation absorption, chemical reaction, hall effects and thermophoresis on all the flow characteristics have been represented graphically.

2.FORMULATION OF THE PROBLEM:

We analyse the transient convective heat and mass transfer flow of an electrically conducting fluid past a stretching sheet with the plane at $y=0$ and the flow is confined to the region $y>0$. A schematic representation of the physical model is exhibited in fig.1. We choose the frame of reference $O(x,y,z)$ such that the x -axis is along the direction of motion of the surface, the y -axis is normal to the surface and z -axis transverse to the $(x-y)$ plane. A uniform magnetic field of strength H_0 is applied in the positive y -direction. The surface of the sheet is assumed to have a variable temperature and concentration $T_w(x)$, and $C_w(x)$ respectively, while the ambient fluid has a uniform temperature and concentration T_∞ and C_∞ , where $T_w(x) > T_\infty$, $C_w(x) > C_\infty$ corresponds to a heated plate and $T_w(x) < T_\infty$, $C_w(x) < C_\infty$ corresponds to a cooling plate. The flow is assumed to be confined in the region $y>0$. We consider a non-uniform internal

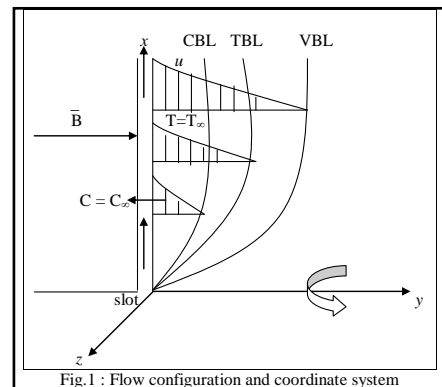


Fig.1 : Flow configuration and coordinate system

heat generation/absorption source in the flow to get the temperature and concentration differences between the surface and ambient fluid. We that the velocity is proportional to its distance from the slit. We consider Hall effects into consideration and assume the electron pressure gradient ,the ion-slip and the thermo-electric effects are negligible.Using boundary layer approximation, Boussinesq's approximation and Rosselang approximation, the basic equations governing the flow,heat and mass transfer in the presence of non-uniform heat source are

$$\frac{\partial u}{\partial x} + \frac{\partial v}{\partial y} = 0 \quad (1)$$

$$\frac{\partial u}{\partial t} + u \frac{\partial u}{\partial x} + v \frac{\partial u}{\partial z} = \nu \frac{\partial^2 u}{\partial y^2} + \beta g(T - T_\infty) + \beta^* g(C - C_\infty) - \frac{\sigma B_0^2}{\rho(1+m^2)}(u + mw) \quad (2)$$

$$\frac{\partial w}{\partial t} + u \frac{\partial w}{\partial z} + v \frac{\partial w}{\partial z} = \nu \frac{\partial^2 w}{\partial y^2} + \frac{\sigma B_0^2}{\rho(1+m^2)}(mu - w) \quad (3)$$

$$\rho C_p \left(\frac{\partial T}{\partial t} + u \frac{\partial T}{\partial x} + v \frac{\partial T}{\partial y} \right) = k_f \frac{\partial^2 T}{\partial y^2} + \frac{k_f U_w(x,t)}{x\nu} (A_1(T_w - T_\infty)f' + (T - T_\infty)B_1) + \quad (4)$$

$$\mu \left[\left(\frac{\partial u}{\partial y} \right)^2 + \left(\frac{\partial w}{\partial y} \right)^2 \right] + Q_1(C - C_\infty) + \frac{16\sigma^* T_\infty^3}{3\beta_R} \frac{\partial^2 T}{\partial y^2}$$

$$\left(\frac{\partial C}{\partial t} + u \frac{\partial C}{\partial x} + v \frac{\partial C}{\partial y} \right) = D_B \frac{\partial^2 C}{\partial y^2} - k_c(C - C_\infty) + \frac{D_m K_T}{T_m} \frac{\partial^2 T}{\partial y^2} - \frac{\partial(V_T C)}{\partial y} \quad (5)$$

The relevant boundary conditions are

$$u = U_w(x,t), L \frac{\partial u}{\partial y}, v = V_w, T = T_w, C = C_w \quad \text{at } y = 0 \quad (6)$$

$$u \rightarrow 0, T \rightarrow T_\infty, C \rightarrow C_\infty \quad \text{as } y \rightarrow \infty \quad (7)$$

Where T is the temperature,C is the concentration inside the boundary layer,u ,v and w sre the velocity components along x,y and z-directions respectively,Cp is the specific heat at constant pressure,Cs is the concentration susceptibility,ρ is the density of the fluid,,kf is the thermal conductivity,μ is the fluid viscosity, ν is the kinematic viscosity,T_w(x,t) is the stretching surface temperature,C_w(x,t) is the concentration of the stretching surface, T_∞ is the temperature far away from the stretching surface with Tw>T_∞ , C_∞ is the concentration far away from the stretching surface with Cw>C_∞ .The term $V_w = -\sqrt{\frac{\nu U_w}{2x}} f(0)$ represents the mass transfer at the surface with V_w>0 for suction and V_w<0 for injection.

Due to stretching of the sheet the flow is caused and it moves with the surface velocity ,temperature and concentration of the form

$$U_w(x,t) = \frac{ax}{1-ct}, T_w(x,t) = T_\infty + \frac{ax}{1-ct}, C_w(x,t) = C_\infty + \frac{ax}{1-ct} \quad (8)$$

where a is stretching rate and c are positive with ct<1,c≥0. It is noticed that the stretching rate $\frac{ax}{1-ct}$ increases with time t since a>0.

The stream function ψ(x,t) is defined as:

$$u = \frac{\partial \psi}{\partial y} = \frac{ax}{(1-ct)} f'(\eta), v = -\frac{\partial \psi}{\partial x} = \frac{av}{(1-ct)} f(\eta) \quad (9)$$

On introducing the similarity variables(Dulal Pal [7]):

$$\eta = \sqrt{\frac{a}{(1-ct)}} y, \quad u = \frac{ax}{1-ct} f'(\eta), v = -\sqrt{\frac{va}{1-ct}} f(\eta), w = \frac{ax}{1-ct} g(\eta), \quad \theta(\eta) = \frac{T-T_\infty}{T_w-T_\infty}, \phi = \frac{C-C_\infty}{C_w-C_\infty} \quad (10)$$

$$B^2 = B_o^2(1-ct)^{-1}$$

where T is the temperature and C is the concentration in the fluid. k_f is the thermal conductivity, C_p is the specific heat at constant pressure, β is the coefficient of thermal expansion, β^* is the volumetric expansion with concentration, Q_1^1 is the radiation absorption coefficient, q_r is the radiative heat flux, kc is the chemical reaction coefficient, D_B is the molecular viscosity, D_m , K_T , T_m mean fluid temperature, k is the porous permeability parameter.

The effect of thermophoresis is usually prescribed by means of average velocity acquired by small particles to the gas velocity when exposed to a temperature gradient. In boundary layer flow, the temperature gradient in the y-direction is very much larger than in the x-direction and therefore only the thermophoresis velocity in y-direction is considered. As a consequence, the thermophoresis velocity V_T , which appears in equation (4) is expressed as

$$V_T = -\frac{k_1 v}{T_r} \frac{\partial T}{\partial y} \quad (11)$$

In which k_1 is the thermophoresis coefficient and T_r is the reference temperature. A thermophoresis parameter τ is given by the relation

$$\tau = -\frac{k_1(T_w - T_\infty)}{T_r} \quad (12)$$

Where the typical values of τ are 0.01, 0.1 and 1.0 corresponding to approximate values of $k_1(T_w - T_\infty)$ equal to 3, 30, 300K for a reference temperature of $T = 300K$

Using Equations (9), (10) & (11) into equations (2), (3) and (5) we get

$$f''' + ff'' - (f')^2 - S(f' - 0.5\eta f'') - \frac{M^2}{1+m^2}(f' + mg) + G(\theta + N\phi) = 0 \quad (13)$$

$$g'' + fg' - f'g - S(g' + 0.5g'') + \frac{M^2}{1+m^2}(mf' - g) = 0 \quad (14)$$

$$\left(1 + \frac{4Rd}{3}\right)\theta'' + Pr(f\theta' - f'\theta) - PrS(\theta + 0.5\eta\theta') + (A_1f' + B_1\theta) + PrEc((f'')^2 + (g')^2) + \frac{EcM^2}{1+m^2}((f')^2 + g^2) + Q_1\phi = 0 \quad (15)$$

$$\phi'' + -Sc(2f'\phi - f\phi') - ScS(\phi + 0.5\eta\phi') + ScSr\theta'' - \tau(\theta'\phi' + \theta''\phi) - Sc\gamma\phi = 0 \quad (16)$$

Where $S = c/a$ is the unsteadiness parameter. $M = \frac{\sigma B_o^2}{\rho a}$ is the magnetic parameter,

$D^{-1} = \frac{\nu}{ak}$ is the inverse Darcy parameter, $G = \frac{\beta g (T_w - T_\infty)}{U_w \nu_w^2}$ is the thermal buoyancy parameter, $N = \frac{\beta^* (C_w - C_\infty)}{\beta (T_w - T_\infty)}$ is the buoyancy ratio, $Pr = \frac{\mu C_p}{k_f}$ is the Prandtl number, $Ec = \frac{U_w^2}{C_p (T_w - T_\infty)}$ is the Eckert number, $Q_1 = \frac{\nu Q_1'}{\nu_w^2}$ is the Radiation absorption parameter, $Sc = \frac{\nu}{D_B}$ is the Schmidt number, $m = \omega_e \tau_e$ is the Hall parameter, $\gamma = \frac{k_o \nu}{\nu_w^2}$ is the chemical reaction parameter and $Sr = \frac{D_m K_T (T_w - T_\infty)}{\nu T_m (C_w - C_\infty)}$ is the Soret parameter.

It is pertinent to mention that $\gamma > 0$ corresponds to a degenerating chemical reaction while $\gamma < 0$ indicates a generation chemical reaction.

The transformed boundary conditions (6)&(10) reduce to

$$\begin{aligned} f'(0) &= 1 + Af''(0), f(0) = fw, \theta(0) = 1, \phi(0) = 1 \\ f'(\infty) &\rightarrow 0, g(\infty) \rightarrow 0, \theta(\infty) \rightarrow 0, \phi(\infty) \rightarrow 0 \end{aligned} \quad (17)$$

Where $fw = \frac{\nu_w}{\sqrt{av}}$ is the mass transfer coefficient such that $fw > 0$ represents suction and $fw < 0$ represents injection at the surface.

3. METHOD OF SOLUTION

The finite element method is a powerful technique for solving ordinary or partial differential equations. The steps involved in the finite element analysis are as follows:

- Discretization of the domain into elements
- Derivation of element equations
- Assembly of element equations
- Imposition of boundary conditions
- Solution of assembled equations

The whole flow domain divided into 1000 quadratic elements of equal size. Each element is three-noded and therefore the whole domain contains 2001 nodes. We obtain a system of equations contains 8004 equations. The obtained system is non-linear, therefore an iterative scheme is utilized in the solution. After imposing the boundary conditions the remaining system contains 7997 equations, which is solved by the Gauss elimination method while maintaining an accuracy of 10^{-5} .

4. IN FRICTION, NUSSELT NUMBER and SHERWOOD NUMBER

The physical quantities of engineering interest in this problem are the skin friction coefficient C_f , the Local Nusselt number (Nu_x), the Local Sherwood number (Sh_x) which are expressed as

$$\frac{1}{2} C_f \sqrt{R_{ex}} = f''(0), \quad \frac{1}{2} C_{fz} \sqrt{R_{ez}} = g'(0), \quad Nu_x / \sqrt{R_{ex}} = 1 / \theta(0), \quad Sh_x / \sqrt{R_{ex}} = 1 / \phi(0)$$

where $\mu = \frac{k}{\rho C_p}$ is the dynamic viscosity of the fluid and R_{ex} is the Reynolds number.

For the computational purpose and without loss of generality ∞ has been fixed as 8. The whole domain is divided into 11 line elements of equal width, each element being three noded.

5.RESULTSAND DISCUSSION:

Comprehensive numerical commutations are conducted for different values of the parameters that describe the flow characteristics and the results are illustrated graphically and in tabular form. Selected graphical profiles are presented in figs.2-9. The comparison of skin friction coefficient $f''(0)$ for values of (Pr) with (33) is made and the results are shown in Table 2 in the absence of other parameters. The results are also compared for Nusselt number $-\theta''(0)$ for various values of (Pr) and α with those of (33,39,40) in the absence of $k, M, Sr, A1, B1, Sc, fw, \tau$ and are presented in table.1. Thus it is seen from table 1 that the numerical results are in close agreement with those published previously.

Figs.2a-2d represent the variation of velocity, temperature and concentration with Hall parameter(m). It can be seen from the velocity profiles that the primary velocity(f') reduces with higher values of Hall parameter(m).while the secondary velocity(g) reduces in the region(0,2.0) and in the region far away from the sheet the secondary velocity enhances with $m > 2.0$ and reduces with smaller values of m . An increase in m enhances the temperature and reduces the mass concentration. This is attributed to the fact that the thickness of the thermal boundary layer increases while the solutal boundary layer thickness decreases with increase in m .

Figs.3a-3d display the influence of chemical reaction parameter (γ) on the velocity, temperature and concentration .It is observed that increasing the chemical reaction parameter reduces the velocities in the degenerating chemical reaction case ($\gamma > 0$) enhances in the generating chemical reaction case($\gamma < 0$).Also an increase in $\gamma > 0$,decreases thickness of thermal and solutal boundary layer and increases with $\gamma < 0$.

The variation of Soret parameter(Sr) on velocities, temperature and concentration are plotted in figs.4a-4d.It is seen from the profiles that the primary and secondary velocities increase with increasing values of the Soret parameter. Higher the thermo-diffusion effects larger the temperature and mass concentration (figs.4c&4d). This may be attributed to the fact the thickness of the thermal and solutal boundary layers increase with increasing Sr .

The influence of unsteadiness parameter (S) on the velocity components, temperature and concentration profiles is shown in figs.5a-5d.It can be seen that the velocity components, temperature decelerates with increase in the values of unsteadiness parameter(S).This is because of the fact that, the motion is generated by the stretching of the sheet and the stretching sheet velocity and temperature is greater than the free stream velocity and temperature, so, the thermal boundary layer thickness decreases with increase in the values of S as shown in fig.5c.The concentration profiles also decreases in the flow region and is shown in fig.5d.It is also observed that the temperature profiles decreases smoothly in the absence of unsteadiness parameter($S=0$) whereas temperature profiles continuously decreases with the increasing values of unsteadiness parameter. This shows that the rate of cooling is much faster for the higher values of unsteadiness parameter and it takes longer time for cooling in the steady flows.

Figs.6a-6d show the variation of velocity, temperature and concentration with space dependent heat source parameter $A1$.The presence of the heat source generates energy in the thermal boundary layer and as a consequence the temperature rises. In case heat absorption($A1 < 0$) the temperature falls with decreasing values of $A1 < 0$ owing to the absorption of energy in the thermal boundary layer. The influence of heat generation is very meagre on the primary velocity when compared to the secondary velocity. In either case both velocities increase with increasing values of heat generating parameter. The effect of heat generation is to enhance the mass concentration marginally.

Figs.7a-7d exhibit the influence of temperature dependent heat source/Sink parameter $B1$ on velocity, temperature and concentration. As in the case of space dependent heat source,

the temperature increases due to the release of thermal energy for $B1 > 0$ while the temperature drops for decreasing values of $B1 < 0$ owing to the absorption of energy. The primary and secondary velocities increase for increasing values of heat source parameter ($B1 > 0$) whereas for $B1 < 0$, the velocities reduce for decreasing values of $B1$. The effect of $B1$ on mass concentration is similar to that of $A1$.

The effect of thermophoresis parameter (τ) on velocity components, temperature and concentration profiles is exhibited in figs.8a-8d. It can be seen from figs.8a&8b that the velocity components depreciate with increase in τ . This is due to the fact that an increase in τ decreases the thickness of the momentum boundary layer. From fig.8c we find that the temperature profiles experience a deceleration with increase in τ . This is because of the fact that the particles near the hot surface create a thermophoretic force. Fig.8d exhibits the impact of τ on concentration profiles, it is noticed that the concentration profiles decrease with increase in thermophoretic parameter (τ). This is because of the fact that the fluid moves from hot surface to the cold surface, then the values of thermophoretic parameter have been taken positive. From these two figures we conclude that the imposition of thermophoretic particles deposition into the flow decreases the thickness of thermal and solutal boundary layers.

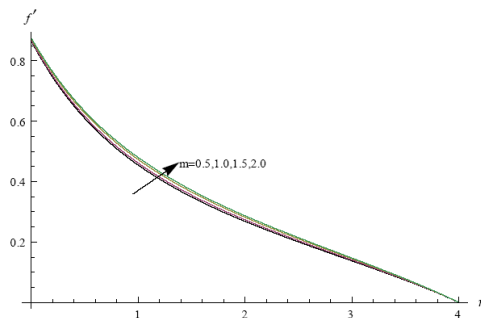


Fig.2a Variation of $f'(\eta)$ with m
 $Sr=0.5, A1=0.1, B1=0.1, S=0.2, A=0.2, \gamma=0.5, \tau=0.1$

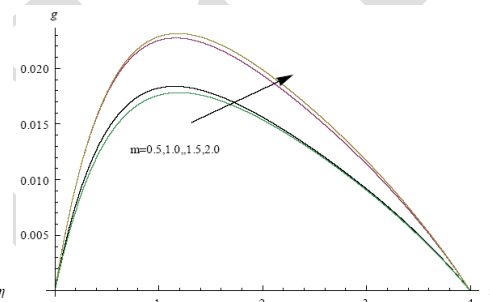


Fig.2b Variation of $g(\eta)$ with m
 $Sr=0.5, A1=0.1, B1=0.1, S=0.2, A=0.2, \gamma=0.5, \tau=0.1$

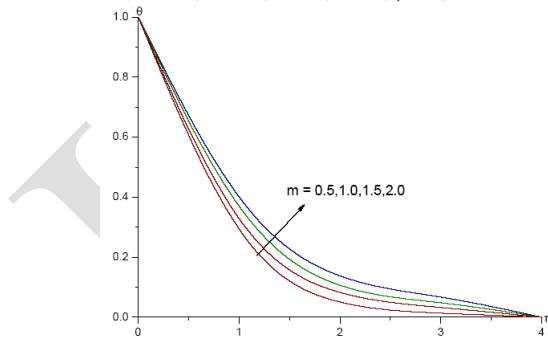


Fig.2c Variation of $\theta(\eta)$ with m
 $Sr=0.5, A1=0.1, B1=0.1, S=0.2, A=0.2, \gamma=0.5, \tau=0.1$

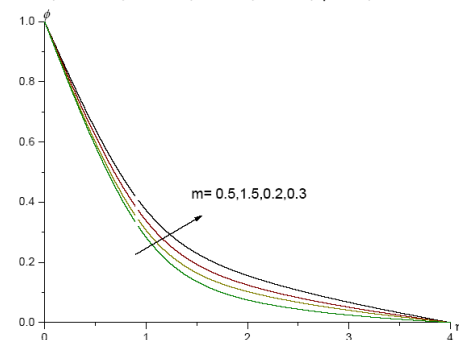


Fig.2d Variation of $\phi(\eta)$ with m
 $Sr=0.5, A1=0.1, B1=0.1, S=0.2, A=0.2, \gamma=0.5, \tau=0.1$

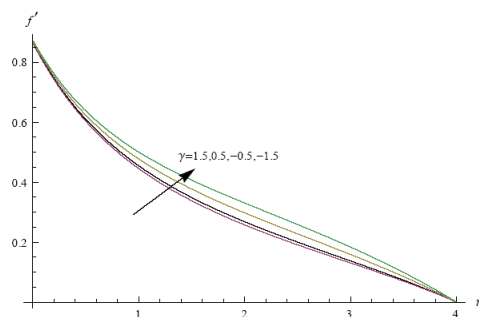


Fig.3a Variation of $f'(\eta)$ with γ
 $m=0.5, Sr=0.5, A1=0.1, B1=0.1, S=0.2, A=0.2, \tau=0.1$

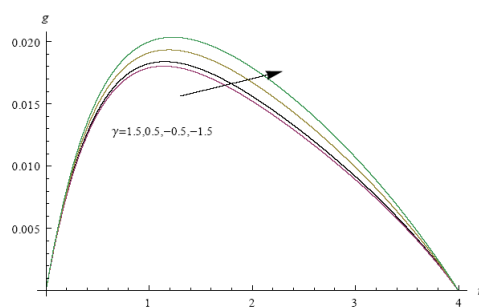


Fig.3b Variation of $g(\eta)$ with γ
 $m=0.5, Sr=0.5, A1=0.1, B1=0.1, S=0.2, A=0.2, \tau=0.1$

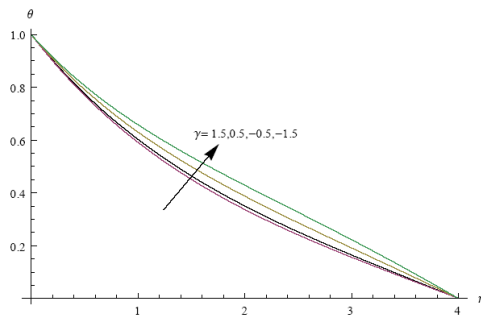


Fig.3c Variation of $\theta(\eta)$ with γ
 $m=0.5, Sr=0.5, A1=0.1, B1=0.1, S=0.2, A=0.2, \tau=0.1$

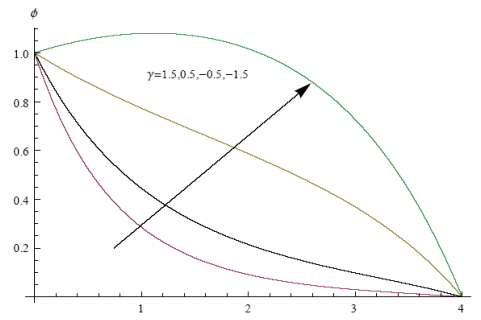


Fig.3d Variation of $\phi(\eta)$ with γ
 $m=0.5, Sr=0.5, A1=0.1, B1=0.1, S=0.2, A=0.2, \tau=0.1$

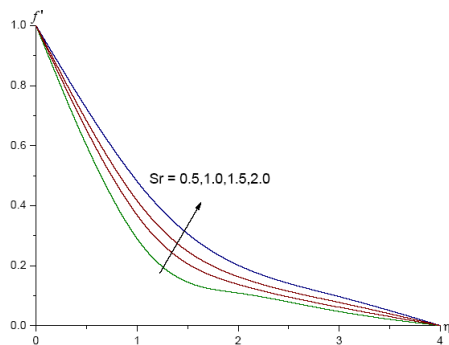


Fig.4a Variation of $f'(\eta)$ with Sr
 $m=0.5, \gamma=0.5, A1=0.1, B1=0.1, S=0.2, A=0.2, \tau=0.1$

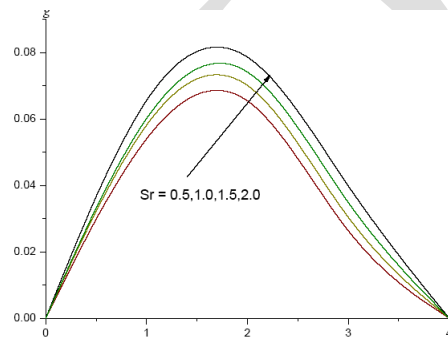


Fig.4b Variation of $g(\eta)$ with Sr
 $m=0.5, \gamma=0.5, A1=0.1, B1=0.1, S=0.2, A=0.2, \tau=0.1$

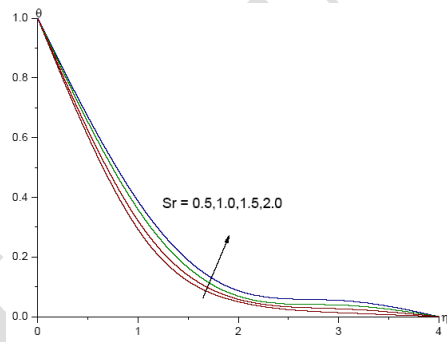


Fig.4c Variation of $\theta(\eta)$ with Sr
 $m=0.5, \gamma=0.5, A1=0.1, B1=0.1, S=0.2, A=0.2, \tau=0.1$

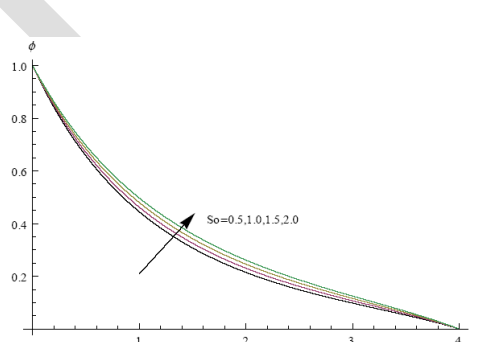


Fig.4d Variation of $\phi(\eta)$ with Sr
 $m=0.5, \gamma=0.5, A1=0.1, B1=0.1, S=0.2, A=0.2, \tau=0.1$

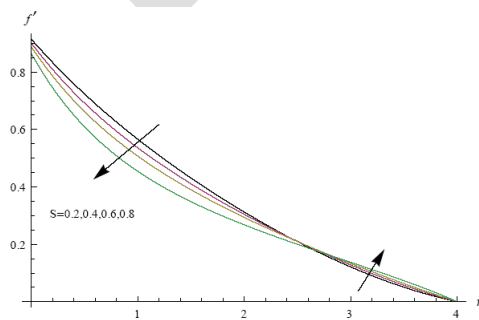


Fig.5a Variation of $f'(\eta)$ with S
 $m=0.5, Sr=0.5, A1=0.1, B1=0.1, \gamma=0.2, A=0.2, \tau=0.1$

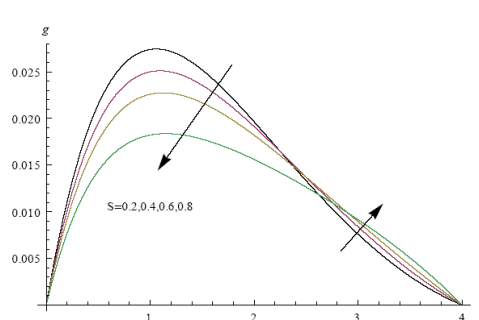


Fig.5b Variation of $g(\eta)$ with S
 $m=0.5, Sr=0.5, A1=0.1, B1=0.1, \gamma=0.2, A=0.2, \tau=0.1$

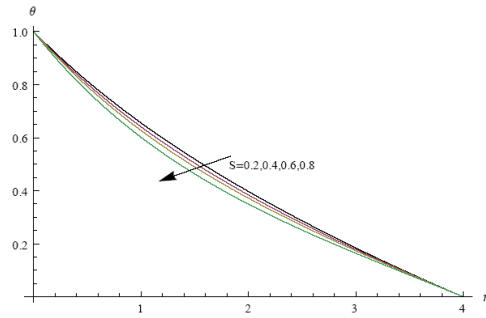


Fig.5c Variation of $\theta(\eta)$ with S
 $m=0.5, Sr=0.5, A1=0.1, B1=0.1, \gamma=0.2, A=0.2, \tau=0.1$

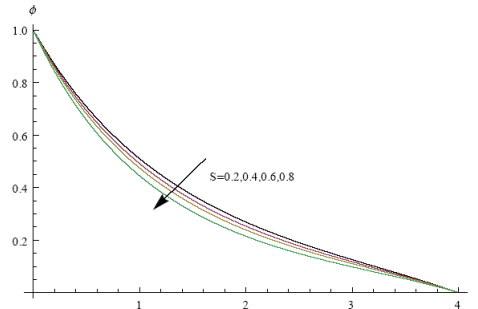


Fig.5d Variation of $\phi(\eta)$ with S
 $m=0.5, Sr=0.5, A1=0.1, B1=0.1, \gamma=0.2, A=0.2, \tau=0.1$

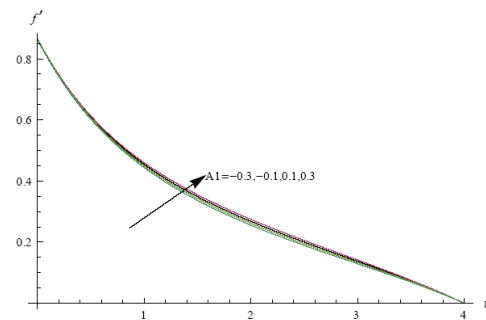


Fig.6a Variation of $f'(\eta)$ with $A1$
 $m=0.5, Sr=0.5, \gamma=0.5, B1=0.1, S=0.2, A=0.2, \tau=0.1$

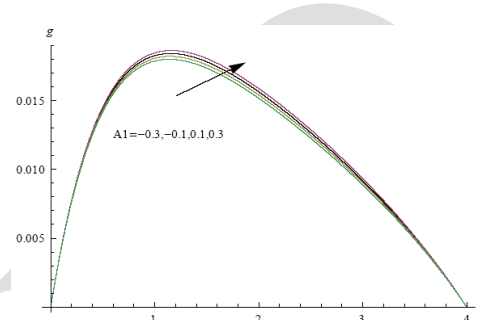


Fig.6b Variation of $g(\eta)$ with $A1$
 $m=0.5, Sr=0.5, \gamma=0.5, B1=0.1, S=0.2, A=0.2, \tau=0.1$

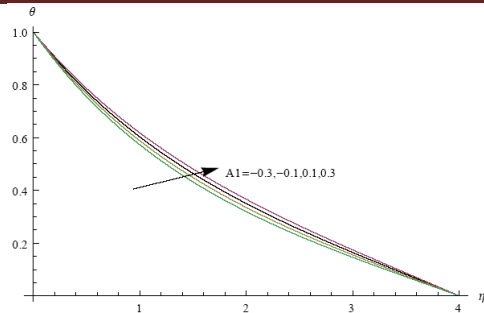


Fig.6c Variation of $\theta(\eta)$ with $A1$
 $m=0.5, Sr=0.5, \gamma=0.5, B1=0.1, S=0.2, A=0.2, \tau=0.1$

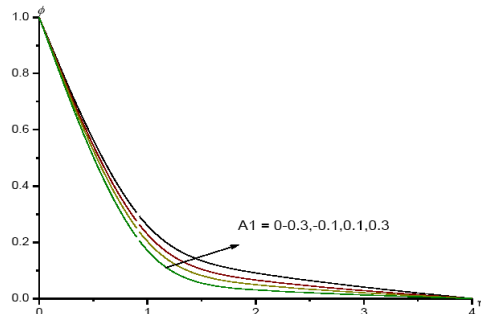


Fig.6d Variation of $\phi(\eta)$ with $A1$
 $m=0.5, Sr=0.5, \gamma=0.5, B1=0.1, S=0.2, A=0.2, \tau=0.1$

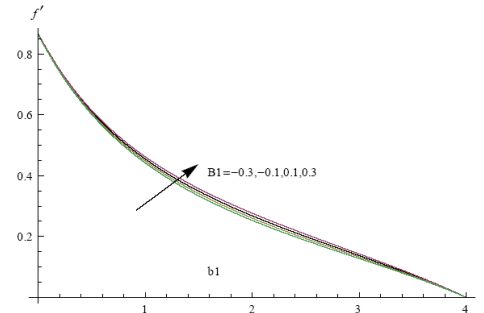


Fig.7a Variation of $f'(\eta)$ with $B1$
 $m=0.5, Sr=0.5, A1=0.1, \gamma=0.5, S=0.2, A=0.2, \tau=0.1$

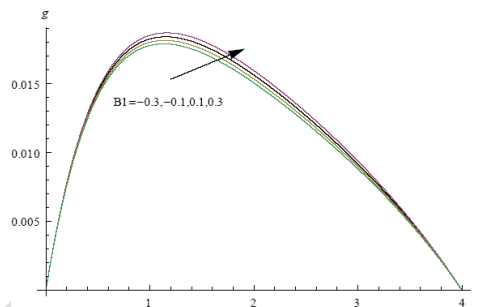


Fig.7b Variation of $g(\eta)$ with $B1$
 $m=0.5, Sr=0.5, A1=0.1, \gamma=0.5, S=0.2, A=0.2, \tau=0.1$

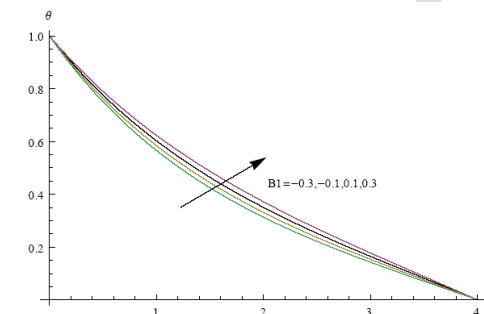


Fig.7c Variation of $\theta(\eta)$ with $B1$
 $m=0.5, Sr=0.5, A1=0.1, \gamma=0.5, S=0.2, A=0.2, \tau=0.1$

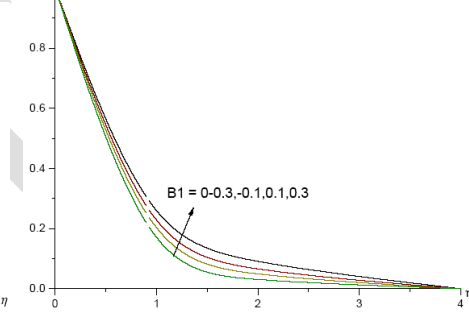


Fig.7d Variation of $\phi(\eta)$ with $B1$
 $m=0.5, Sr=0.5, A1=0.1, \gamma=0.5, S=0.2, A=0.2, \tau=0.1$

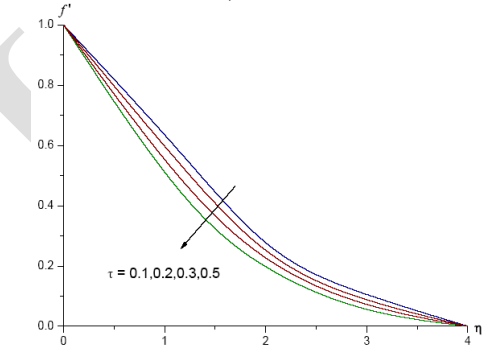


Fig.8a Variation of $f'(\eta)$ with τ
 $m=0.5, Sr=0.5, A1=0.1, B1=0.1, S=0.2, A=0.2, \gamma=0.1$

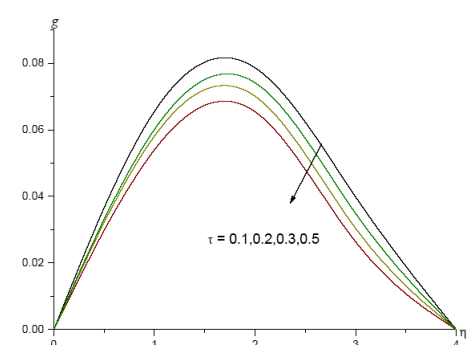


Fig.8b Variation of $g(\eta)$ with τ
 $m=0.5, Sr=0.5, A1=0.1, B1=0.1, S=0.2, A=0.2, \gamma=0.1$

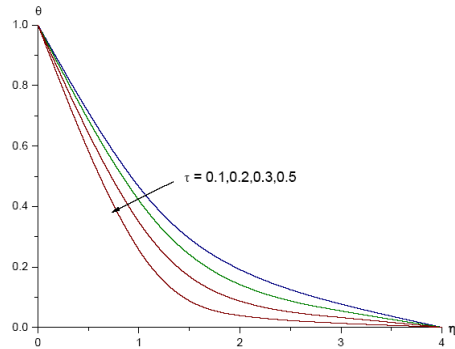


Fig.8c Variation of $\theta(\eta)$ with τ
 $m=0.5, Sr=0.5, A1=0.1, B1=0.1, S=0.2, A=0.2, \gamma=0.1$

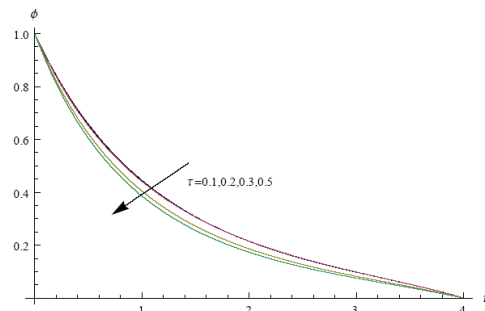


Fig.8d Variation of $\phi(\eta)$ with τ
 $m=0.5, Sr=0.5, A1=0.1, B1=0.1, S=0.2, A=0.2, \gamma=0.1$

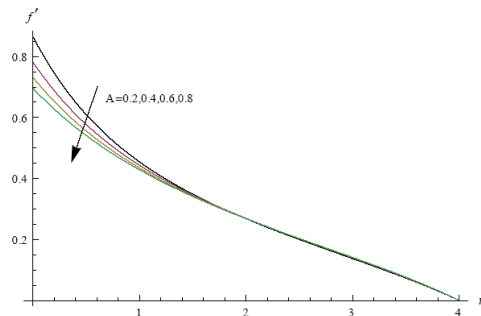


Fig.9a Variation of $f'(\eta)$ with A
 $m=0.5, Sr=0.5, A1=0.1, B1=0.1, S=0.2, \tau=0.1, \gamma=0.1$

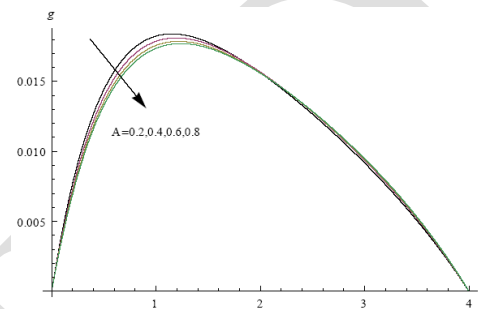


Fig.9b Variation of $g(\eta)$ with A
 $m=0.5, Sr=0.5, A1=0.1, B1=0.1, S=0.2, \tau=0.1, \gamma=0.1$

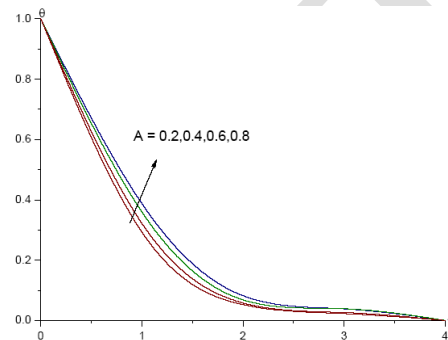


Fig.9c Variation of $\theta(\eta)$ with A
 $m=0.5, Sr=0.5, A1=0.1, B1=0.1, S=0.2, \tau=0.1, \gamma=0.1$

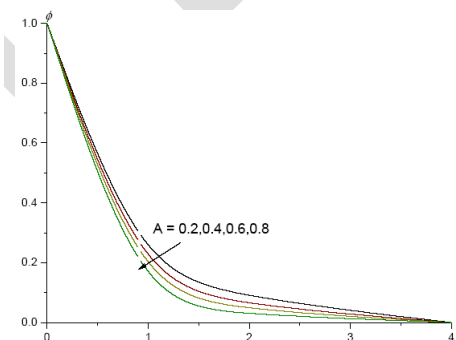


Fig.9d Variation of $\phi(\eta)$ with A
 $m=0.5, Sr=0.5, A1=0.1, B1=0.1, S=0.2, \tau=0.1, \gamma=0.1$

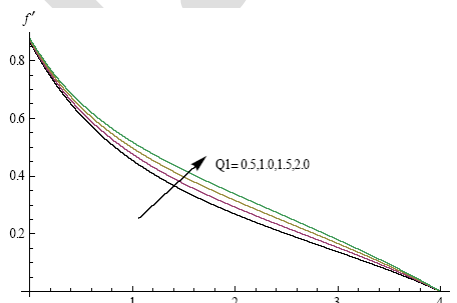


Fig.10a Variation of $f'(\eta)$ with $Q1$
 $m=0.5, Sr=0.5, A1=0.1, B1=0.1, S=0.2, A=0.2, \tau=0.1$

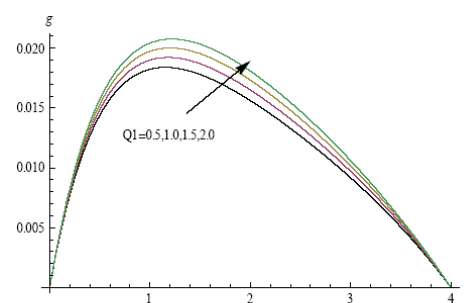


Fig.10b Variation of $g(\eta)$ with $Q1$
 $m=0.5, Sr=0.5, A1=0.1, B1=0.1, S=0.2, A=0.2, \tau=0.1$

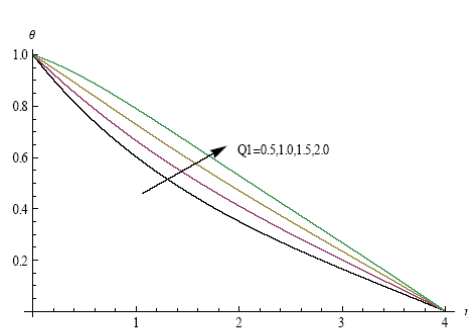


Fig.10c Variation of $\theta(\eta)$ with $Q1$
 $m=0.5, Sr=0.5, A1=0.1, B1=0.1, S=0.2, A=0.2, \tau=0.1$

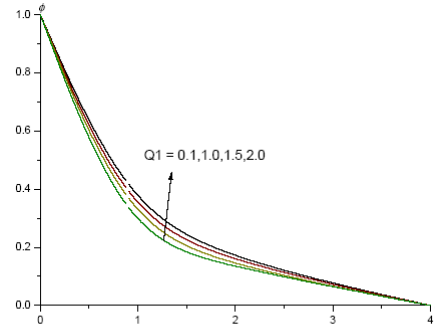


Fig.10d Variation of $\phi(\eta)$ with $Q1$
 $m=0.5, Sr=0.5, A1=0.1, B1=0.1, S=0.2, A=0.2, \tau=0.1$

Figs.9a-9d demonstrate the influence of slip parameter (A) on the velocity, temperature and concentration. It can be seen from the profiles that an increase in the slip parameter (A) reduces the primary and secondary velocities. The temperature rises and the mass concentration drops with increasing values of A .

Fig.10a-10d illustrates the influence of radiation absorption on the velocity, temperature and mass concentration. From the velocity profiles we find that higher the radiation absorption larger the thickness of the momentum boundary layer which results in an enhancement in the primary and secondary velocity components. Also the temperature and mass concentration experience an enhancement with increase in $Q1$ (figs.10c&10d).

The skin friction components (τ_x, τ_y), Nusselt number (Nu) and Sherwood number (Sh) for different Sr, τ, A, S . An increase in Hall parameter (m) reduces the skin friction component τ_x , Sh and enhances τ_y , Nusselt number on the wall. When the molecular buoyancy force dominates over the thermal buoyancy force the skin friction component τ_x and Sh reduces while τ_y and Nu increases when the buoyancy forces are in the same direction and for the forces acting in opposite directions, τ_x, Sh increase, while τ_y, Nu decrease on the wall. Higher the thermo-diffusion effects/radiation absorption effects/thermal radiation/dissipative force, smaller τ_x, Nu and Sh and larger τ_y on the wall. With respect to chemical reaction parameter (γ), we find that τ_x, Nu and Sh enhance while τ_y reduces on the wall in both degenerating and generating chemical reaction cases. An increase in space dependent heat source parameter smaller τ_x, Nu, Sh and larger τ_y on the wall. Decreasing values of $A < 0$, reduces τ_x, Nu, Sh and enhances τ_y on the wall. An increase in $B1 > 0$ reduces τ_x, Nu and Sh while τ_y enhances on the wall. For decreasing values of $B1 < 0$, we notice an enhancement in τ_x, τ_y, Nu and Sh on the wall. Higher the thermophoretic parameter (τ) larger τ_x, Nu and Sh and smaller τ_y on the wall. An increase in the slip parameter (A) reduces the skin friction components and Nusselt number and enhances the Sherwood number on the wall. The skin friction component τ_x , rate of heat and mass transfer on the wall experience an enhancement with increasing values of unsteadiness parameter S while τ_y reduces with S . τ_x, τ_y enhance and Nu, Sh reduce with increase in Suction/injection parameter (fw).

Table 1 : Skin friction (τ_x), Nusselt Number (Nu) at $\eta = 0$

Parameter		$\tau_x(0)$	$\tau_z(0)$	Nu(0)	Sh(0)
m	0.5	-0.6735	0.04712	0.51352	0.87656
	1.0	-0.6614	0.05745	0.51472	0.87637
	1.5	-0.6364	0.05725	0.51738	0.87595
	2.0	-0.5652	0.06733	0.59696	0.83909
A1	0.1	-0.6735	0.04741	0.51352	0.87656
	0.3	-0.6678	0.04738	0.48474	0.87453
	-0.1	-0.6778	0.04683	0.54048	0.87848
	-0.3	-0.6355	0.045023	0.54794	0.84411
B1	0.1	-0.6735	0.04714	0.51352	0.87656
	0.3	-0.6662	0.04747	0.47656	0.87391
	-0.1	-0.6791	0.04676	0.54711	0.87895
	-0.3	-0.6323	0.05021	0.55926	0.84492
γ	0.5	-0.6735	0.04714	0.51352	0.87656
	1.5	-0.6822	0.04661	0.52784	1.33301
	-0.5	-0.6335	0.04948	0.44978	0.14601
	-1.5	-0.7204	0.04302	0.59288	0.53271
Sr	0.5	-0.6735	0.04714	0.51352	0.87656
	1.0	-0.6727	0.04711	0.51312	0.86622
	1.5	-0.6722	0.04685	0.51191	0.83535
	2.0	-0.6175	0.04595	0.48876	0.78477
S	0.1	-0.4251	0.06536	0.40831	0.71332
	0.3	-0.4934	0.06016	0.43626	0.75755
	0.5	-0.5586	0.05531	0.46321	0.79967
	0.7	-0.6191	0.05086	0.49104	0.84002
τ	0.1	-0.6735	0.04741	0.51352	0.87656
	0.2	-0.6742	0.04703	0.51541	0.94482
	0.3	-0.6753	0.04698	0.51711	1.00927
	0.5	-0.6827	0.04566	0.53645	1.02977
A	0.2	-0.6735	0.0471	0.51352	0.87656
	0.4	-0.5206	0.04448	0.50534	0.87848
	0.6	-0.4326	0.04294	0.50043	0.87963
	0.8	-0.3421	0.04159	0.47537	0.88371
Q1	0.5	-0.673	0.0471	0.51352	0.87656
	1.0	-0.6677	0.04738	0.48148	0.87428
	1.5	-0.652	0.0482	0.38544	0.86749
	2.0	-0.6419	0.04872	0.32307	0.86309

6. CONCLUSIONS:

The non-linear equations governing the flow heat and mass transfer have been solved by using Runge-Kutta Shooting technique. From the graphical representations and tabular values we find that

- The velocity profiles that the primary velocity(f') reduces with higher values of Hall parameter(m). while the secondary velocity(g) reduces in the region $(0, 2.0)$ and in the region far away from the sheet the secondary velocity enhances with $m > 2.0$ and reduces with smaller values of m . An increase in m enhances the temperature and reduces the mass concentration.
- The velocity profiles we find that higher the radiation absorption larger the thickness of the momentum boundary layer which results in an enhancement in the primary and secondary velocity components. Also the temperature and mass concentration experience an enhancement with increase in Q_1 .
- Higher the thermo-diffusion effect larger the velocities, and concentration and smaller the temperature in the flow region. The rate of heat and mass transfer reduces with S_r .
- An increase in Thermophoresis parameter(τ) reduces velocities, temperature and concentration. The Nusselt and Sherwood number on the wall enhance with increase in τ .
- An increase in slip parameter(A) reduces the velocities, concentration and enhances the temperature. The Nusselt number reduces and the Sherwood number enhances with increase in A .

7. REFERENCES

- [1]. Abo-Eldahab E.M., and El-Gendy M.S. : Heat current and ohmic heating effect on mixed convection boundary layer flow of amicropolar fluid from a rotating cone with power-law variation in surface temperature, *Int. Commun.HeatMass Transfer*, 31,751-762, 2004.
- [2]. Ali, M.E. : Heat transfer characteristics of a continuous stretching surface, *Heat mass transfer*, 29, 227-234, (1994).
- [3]. Aliveli B, Sreevani M : Convective heat and mass transfer flow of viscous fluid with variable viscosity in the presence of thermophoresis particle deposition, *International Journal for Research & Development in Technology*, Vol.8, Issue 5 (2017), Issn 2349-3585, web.www.ijrdt.org.
- [4]. Chamkha A.J, and Rashad A.M.: Unsteady heat and mass transfer by MHD mixed convection flow from a rotating vertical cone with chemical reaction and Soret and Dufour effects, *The Canadian Journal of Chemical Engineering*, DOI 10.1002/cjce 21894, (2014).
- [5]. Crane, L.J., Z. Angew: Flow past a stretching plate, *Math. Phys*, 21, pp. 645–647 (1970).
- [6]. Damseh R.A., Tahat M.S, and Benim A.C, Non-similar solutions of magnetohydrodynamic and thermophoresis particle deposition on mixed convection problem in porousmedia along a verticalsurface with variable wall temperature, *Progress in Computational Fluid Dynamics* 9(1), 58-65, (2009).
- [7]. Dulal Pal, and Mondal. H, MHD non-Darcian mixed convection heat and mass transfer over a non-linear stretching sheet with Soret and Dufour effects and chemical reaction, *International communications in heat and mass transfer*, 463-467 (2011).
- [8]. Duwairi H.M., Damseh R.A., Effectof thermophoresis particle deposition on mixed convection from vertical surfaces embedded in saturated porousmedium, *Int. J.Numerical Methods Heat Fluid Flow*, 18(2), 202-216 (2008).

- [9]. Grubka L.G. and Bobba K.M., Heat transfer characteristics of a continuous stretching surface with variable temperature, J.Heat Transfer – Trans. ASME.107, P.248-250 (1985)
- [10]. Gupta, P.S., Gupta, A.S: Heat and Mass Transfer on a stretching sheet with suction or blowing, can.J.Chem.Eng, 55, pp. 744-746 (1977).
- [11]. Mahdy A, Hady f.M., Effect of thermophoretic particle deposition in non-Newtonian free convection flow over a vertical plate with magnetic field effect, Journal of Non-Newtonian fluid Mechanics, 161 (1-3), 37-41 (2009).
- [12]. Makinde, O.D, On MHD Mixed Convection with Soret and Dufour Effects Past a Vertical Plate Embedded in a Porous Medium, Latin American Applied Research 42, 63-68 (2011).
- [13]. Mansour M.A., and El-Shaer N.A., Radiative effects on magnetohydrodynamic natural convection flows saturated in porous media, J. Magn.Mater, 237,327-341, (2001).
- [14]. Molla Md. M, Saha S.C., and Hossain Md.A : Radiation effect on free convection laminar flow along a vertical flat plate with stream wise sinusoidal surface temperature, Math. Comput. Modeling, 53,1310-1319, (2011).
- [15]. Pal D, Heat and mass transfer in stagnation-point flow towards a stretching surface in the presence of buoyancy force and thermal radiation, Meccanica, 44,145-158, (2005).
- [16]. Pal. D, and Mandal H, The influence of thermal radiation on hydromagnetic Darcy-Forchheimer mixed convection flow past a stretching sheet embedded in a porous medium, Meccanica, doi:10.1007/s 11012-010-9334-8, (2010)
- [17]. Plumb O.A., Huenfield J.S., and Eschbach E.J., The effect of cross flow and radiation on natural convection from vertical heated surfaces in saturated porous media, in : AIAA 16th Thermophysics conference, June 23-25, Palo Alto, California, USA, (1981).
- [18]. Reddy P.S. and Rao V.P. : Thermo-Diffusion and Diffusion – Thermo Effects on Convective Heat and Mass Transfer through a Porous Medium in a Circular Cylindrical Annulus with Quadratic Density Temperature Variation – Finite Element Study, Journal of Applied Fluid Mechanics, 5(4), 139-144, (2012).
- [19]. Sikiadis B.C., Boundary layer behavior on continuous solid surfaces, IChE J.7, 26-28, (1961)
- [20]. Sivagopal R, Siva Prasad R : Soret and Dufour effects on MHD heat and mass transfer flow of a micropolar fluid over stretching sheet through porous medium with thermo-phoresis, *International Journal of Advanced Scientific and Technical Research* ,Issue 6 volume 5, September-October 2016 web: www.rspublication.com, ISSN:2249-9954, Impact Factor 3.6.
- [21]. Sreenivasa Reddy B, Madhusudhana K and Sreedhar Babu M : The effect of thermoporosity on convective heat and mass transfer flow past stretching sheet with Soret and Dufour effect, International Research Journal of Mathematics, Engineering and I.T., Vol.3(6), (2015).
- [22]. Talbot L, Cheng R.K., Schefer R.W., and et al, Thermophoresis of particles in a heated boundary layer. J. FluidMech, 101(4), 737-758, (1980)
- [23]. Tsou, F.K., Sparrow, E.M. and Goldstein, R.J: Flow and heat transfer in the boundary layer on a continuous moving surface, Int. J. Heat Mass Transfer 10, pp. 219–235 (1967).
- [24]. Vajravelu K, and Rollis D : Heat transfer in electrically conducting fluid over a stretching surface, Internat. J. Non-linear mech, 27(2), 265-277, (1992)

-
- [25]. Vajravelu, K, Flow and heat transfer in a saturated over a stretching surface, ZAMM. V. 74, pp. 605-614, (1994).
[26]. Wang CY : Stretching a surface in a rotating fluid, ZAMP 39; 177-185, (1988).